COUPLING SELECTIVE CATALYTIC REDUCTION PROCESS INSIDE A COKE OVEN REGENERATOR
The Influence of Mixing Parameters on NO Reduction

by

Wei BAI[a], Jun-Xiao FENG[a,b], Yu-Jie ZHAO[a], and Huan-Bao FAN[a]*

[a] School of Energy and Environmental Engineering,
University of Science and Technology, Beijing, China
[b] Beijing Key Laboratory for Energy Conservation and Emission Reduction in Metallurgical industry,
Beijing, China

Many coking plants have adopted the process of preheating flue gas to apply medium and low temperature selective catalytic reduction (SCR) denitrification technology, which increases the NO_x treatment cost, fuel consumption, and generates secondary pollutants. Based on the unique temperature distribution characteristics of the coke oven regenerator, this work proposes a method for synergizing SCR inside the regenerator to remove NO_x. A 3-D numerical model of the synergy between heat storage and SCR reaction was constructed to study the influence of mixing parameters (atomization angle, injection velocity, nozzles number) on the NO reduction and NH_3 distribution. The validity of the model was verified. The results showed that the uneven distribution of NH_3 near the catalytic layer and the small SCR coating area limited the NO reduction efficiency. Increasing the number of nozzles was more beneficial than the injection velocity and atomization angle for improving the NH_3 distribution uniformity and NO reduction efficiency, achieving a maximum NO reduction efficiency of 37.1% (reduced to 251.6 mg/m^3). Further research found that the NO reduction capacity of the co-operative SCR model cannot exceed 36% without changing the thermal storage brick structure. When the inlet NO concentration is less than 235 mg/m^3, the reaction model ensures that the outlet NO concentration meets the national emission standards.

Key words: *selective catalytic reduction, coke oven regenerator, NO reduction, coupling process, numerical simulation, uniformity distribution*

Introduction

Modern regenerative coke oven systems include a carbonization chamber, combustion chamber, and regenerator [1]. The combustion process of blast furnace gas or coke oven gas generates a high NO_x concentration of 400~1000 mg/m^3 [2, 3]. Flue gas discharged from a coke oven directly into the atmosphere without treatment causes serious harm to the environment and human health. The Chinese environmental protection department issued and implemented pollutant emission standards requiring that NO_x in unique regions be less than 150 mg/m^3. This brings enormous environmental pressure to currently running and to-be-built

4572

Bai, W., *et al.*: Coupling Selective Catalytic Reduction Process inside a Coke ...
THERMAL SCIENCE: Year 2022, Vol. 26, No. 6A, pp. 4571-4582

coking enterprises. Considering the strictness of current and future environmental protection standards, coking companies must urgently develop new technologies to control NO_x emissions.

Coke oven flue gas NO_x control methods include combustion mode improvement and combustion post-treatment. Improving the combustion mode declines the local high temperature, weakening the production of thermal and rapid NO_x [4, 5]. Among them, methods such as external flue gas circulation [6], staged combustion [3], and oxygen-enriched fuel [7] were used to reduce the generation of NO in coke oven flue gas. However, in terms of achieving emission standards, this approach needs further exploration. The post-treatment SCR process selectively reacts to the reducing agent (NH_3 or urea) with NO_x to generate N_2 and H_2O [8]. Owing to its many advantages (*i.e.*, high NO reduction efficiency, compact equipment, and reliable operation) [9], the post-treatment SCR process has been accepted by most coking companies. The denitration efficiency of the SCR system depends on whether the flue gas and NH_3 are mixed well in the reactor. There have been many reports about enhancing the uniformity of NH_3 distribution improve NO reduction. One way is to improve the uniformity of the flow field by setting up deflectors, rectifier grids, and other structures [10-15]. Another way is to enhance uniformity at the SCR catalytic zone entrance by changing the operating parameters (*i.e.*, atomization angle, injection position, injection method, and injection velocity) [16, 17]. The SCR technology used in coking plants generally achieves a NO reduction of over 90%. However, there are many problems in these practical applications. Firstly, considering the vulnerability of SCR catalysts that are easily poisoned and non-renewable [18], enterprises face difficulties selecting the desulfurization and denitration sequence in the flue gas treatment system. Secondly, since the mainstream SCR catalyst has a working temperature window of 300~400 °C [19-21], installing a supplementary heating device is necessary to increase the flue gas temperature (180~230 °C). This result added to enterprises' economic investment, brought additional fuel consumption, and simultaneously produced secondary pollution. Many scholars have experimented with low temperature SCR catalysts [8, 22-24]. However, limited by the operating conditions, there have been few cases of application in flue gas systems [25, 26].

Therefore, the economic costs and fuel consumption problems caused by applying medium and low temperature SCR denitration coking plants must be solved urgently. Currently, there are few reports on applying SCR to coke oven heating systems. To solve the problems mentioned previously in the NO_x treatment of coking flue gas, this work combines the temperature distribution characteristics of the regenerator [27] and proposes a new-type regenerator synergistic SCR process. In this study, a suitable temperature window was selected as the coating area of the vanadium-based SCR catalyst. The flow, heat and mass transfer, and NO reduction effect of the cooperative SCR inside the regenerator were numerically studied. The validity of the SCR reaction model was verified. The influence of mixing parameters (atomization angle, injection velocity, nozzles number) and inlet NO concentration on NO_x emission reduction was analyzed. The research provides a parameter index and theoretical basis for the synergy SCR process inside the regenerator to replace the medium and low temperature SCR denitration system.

Modelling and methodology

The geometric model of the regenerator synergistic SCR process

A traditional coke oven regenerator consists of nine-hole checker bricks stacked in sequence, fig. 1(a). To realize the co-operative SCR process application in the regenerator, based on the traditional structure, we removed part of the checker bricks inside the regenerator to leave a specific space (called the NH_3 injection space) for the reductant injection. The mod-

Bai, W., *et al.*: Coupling Selective Catalytic Reduction Process inside a Coke ...
THERMAL SCIENCE: Year 2022, Vol. 26, No. 6A, pp. 4571-4582

4573

ified structure of the new-type regenerator is shown in fig. 1(b). It was assumed that the active component V_2O_5/TiO_2 uniformly coated the wall of the flue gas channels in part CD for the SCR catalytic reaction. The velocity, temperature, and component concentration distribution at the model entrance were uniform.
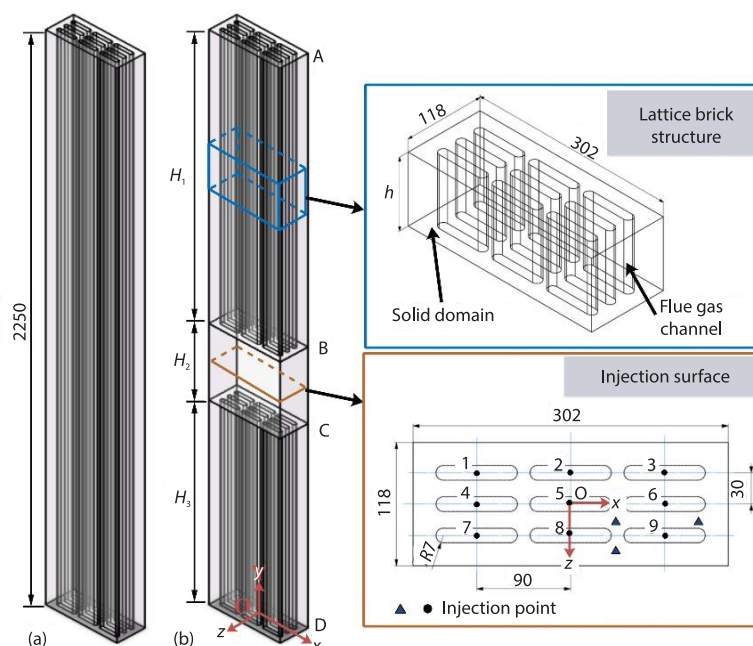

Figure 1. The structure of the new-type regenerator and the SCR implementation method; (a) the structure of the traditional regenerator and (b) the structure of the new regenerator

According to the characteristics of space axis symmetry, a quarter of the 3-D regenerator model cooperative SCR process was established for numerical calculation. We assumed that the height of the regenerator was 2250 mm. The cross-sectional dimension of the NH_3 injection space was 302×118 mm. The temperature distribution determined the position of the NH_3 injection space H_{BC} and the SCR coating area H_{CD}. We assumed that the coating area was filled with the medium-low temperature section during the initial calculation. The structural parameters of the new regenerator of the cooperative SCR process were: AB section height $H_1 = 1150$ mm, BC section height $H_2 = 300$ mm, and CD section height $H_3 = 800$ mm.

Governing equation

The flow, heat and mass transfer, and chemical reactions were considered in the numerical model and calculated using FLUENT platform (ANSYS, Inc., Canon-sburg, Penn., USA). The NH_3 injection space in the geometric model affected the flow state, so the RNG k-ε turbulence model was selected to manage low Reynolds number and near-wall flow [28]. The regenerative coupled SCR process includes delayed flow, heat transfer, component evaporation and SCR catalytic reaction. The corresponding governing equations of this process have been described in previous work [29, 30].

We verified that thermal radiation had a minimal effect on the temperature distribution inside the regenerator [27]. On the other hand, the radiation effect produced by the injection stream was also weak [31]. Therefore, the thermal radiation was ignored in this simulation.

Discrete phase modelling (DPM) described the heat and mass transfer caused by the NH_3 injection. The chemical equilibrium equation of the NO reduction reaction considered in this work:

$$4NO + 4NH_3 + O_2 \rightarrow 4N_2 + 6H_2O \tag{1}$$
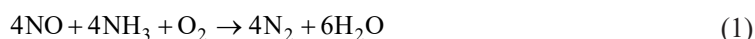
The SCR reaction kinetic model and rate expression used in the model [18, 32] are described:

$$r_{NO} = k_{NO}c_{NO}\theta_{NH_3} \tag{2}$$

$$\theta_{NH_3} = \frac{Kc_{NH_3}}{1 + Kc_{NH_3}}, \quad k_{NO} = A_{NO}\exp^{\frac{-E_{a,NO}}{RT}}, \quad K = A_{ads}\exp^{\frac{\Delta H_{ads}}{RT}} \tag{3}$$

where k_{NO} is the intrinsic reaction rate constant, c_i – the concentration of i species, i = NO, NH_3, θ_{NH3} – the coverage of NH_3 on the catalyst, K – the NH_3 adsorption equilibrium constant on the catalyst, A_{NO} and $E_{a,NO}$ are the pre-exponential factor and activation energy in the Arrhenius equation, A_{ads} and ΔH_{ads} – the pre-exponential factor and NH_3 adsorption heat in NH_3 adsorption equation.

The SCR reaction kinetic model parameters shown in tab. 1 were obtained through experiments [21]. The experiments were conducted in a benchtop reactor using a commercial V_2O_5/TiO_2 catalyst, and the reaction temperature was between 320~400 °C.

Table 1. Kinetic parameters of the SCR reaction

Parameters	Value	Unit
A_{NO}	$3.17 \cdot 10^6$	[s^{-1}]
$E_{a,NO}$	50.38	[kJmol^{-1}]
A_{ads}	$2.55 \cdot 10^{-10}$	[m^{3}mol^{-1}]
ΔH_{ads}	153.23	[kJmol^{-1}]

Solving conditions

The data for this work was derived from a JNK43-98D coke oven in a coking plant. The height of the carbonization chamber in the JNK43-98D is 4.3 m, and each carbonization chamber corresponds to two regenerators. This coke oven has dual fire channels and exhaust gas circulation, it also has the advantages of a long life, environmental protection, and low investment [33]. The mass-flow rate of the high temperature flue gas-flowing from the upstream of the regenerator into the geometric model is 0.0075 kg/s, and the outlet was the pressure boundary.

Relevant data were collected at the operation site of the coke oven [27]. The volume fraction of the main components of the flue gas was measured before entering the chimney: CO_2/0.206, O_2/0.054, H_2O/0.057, N_2/0.685, and the NO_x concentration was 400 mg/m^3. Furthermore, the prediction equation $T_{in} = 1342.391 + 0.02294t$ was obtained between the inlet temperature T_{in} and the heat storage time t.

The droplet size in the DPM model conformed to the Rosin-Rammler distribution. A solid-cone nozzle was used to inject NH_3-water, and the initial conditions were set, as shown in tab. 2.

Bai, W., *et al.*: Coupling Selective Catalytic Reduction Process inside a Coke ...
THERMAL SCIENCE: Year 2022, Vol. 26, No. 6A, pp. 4571-4582

4575

Table 2. Initial parameters of NH₃-water injection

Parameters	Value	Unit
Temperature	300	[K]
Velocity	0.1	[ms^{-1}]
NH$_3$ concentration	0.09	[wt.%]
Atomization angle	40	[°]
Average particle size	100	[μm]
Diameter of injection point	0.18	[mm]

Mesh division

The coupled heat transfer between the flue gas and regenerator was considered in the model. The mesh of the fluid area and the solid area were divided separately. It was a hybrid grid consisting of hexahedral grids. Mesh refinement was conducted on the boundary of the fluid domain to improve the accuracy of the numerical simulation. In addition, the independence of the grid was verified. Because when the number of grids is greater than 580000 grid cells, the monitored outlet temperature and composition NO/NH$_3$ remain basically unchanged. Therefore, 580000 grids were finally selected for calculatio. Mesh independence verification and meshing results were presented in previous work [29]. The SIMPLE algorithm was used to solve the momentum equation's pressure-velocity coupling problem. The second-order central difference scheme solved the convection term and diffusion term in the governing equation, and the calculation criterion of the equation was 10^{-6}.

Results and discussion
Model verification of SCR catalytic reaction

In this study, the SCR reaction mechanism and related parameters proposed by Zheng *et al.* [34] were used to verify the model's validity. The data provided by this literature include: N/1000 ppm, NH$_3$/750 ppm. Figure 2 depicts the NO conversion efficiency gradually increasing with the reaction temperature. The comparison between the simulation results in the temperature range of 320~400 °C and the experimental reference data show that the SCR reaction catalyst model established in this work simulates the experimental conditions well. The maximum deviation did not exceed 7.5%. Therefore, the established model was effective in simulating the SCR reaction process.
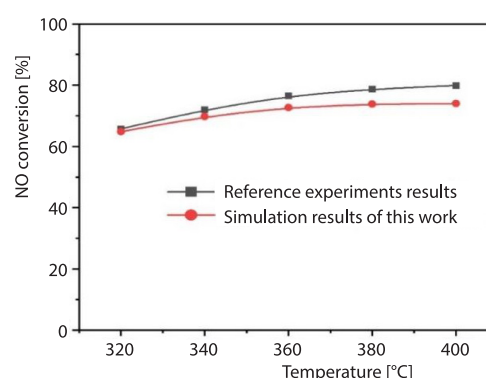

Figure 2. Experimental and simulation results of NO conversion at different temperatures

Analysis of velocity, temperature and NO reduction of the SCR process

In this section, to investigate the concentration distribution of NO and NH$_3$ in the *x*-direction, the edges of the flue gas channel with a cross-section of $Y = 0$~500 mm are named *Symmetry-surface*, *Wall surface-1*, *Wall surface-2*, and *Wall surface-3*.

4576

Bai, W., *et al.*: Coupling Selective Catalytic Reduction Process inside a Coke ...
THERMAL SCIENCE: Year 2022, Vol. 26, No. 6A, pp. 4571-4582

Figure 3(c) shows a prominent NH_3 concentration peak in the NH_3 injection space. When the injection flow of 0.1 m/s mixed with the incoming smoke of 0.8~1.2 m/s, the velocity difference caused most of the NH_3 to be confined to flow into the channels of the middle-low temperature section, and a small part of the injection flow spread locally to the cross-section. As a result, the NH_3 concentration near the walls of the *Wall surface-1* and *Wall surface-2* areas was low and unevenly distributed. The SCR catalytic reaction described in fig. 3(d) had a strong correlation with the temperature near the wall. Affected by the regenerator temperature and NH_3 distribution, the NO reduction at *Wall surface-3* occurred earlier and more extensively than at *Wall surface-1*, and *Wall surface-2*.

The SCR process gradually reduced the NO concentration from 397 mg/m³ at the height $Y = 500$ mm to 263 mg/m³ at the outlet ($Y = 0$ mm), achieved a NO reduction efficiency of 34.2%. In the case of sufficient NH_3, the monitored outlet NO maintained a higher concentration. This may be caused by the inadequate NH_3 distribution and small SCR catalytic area.
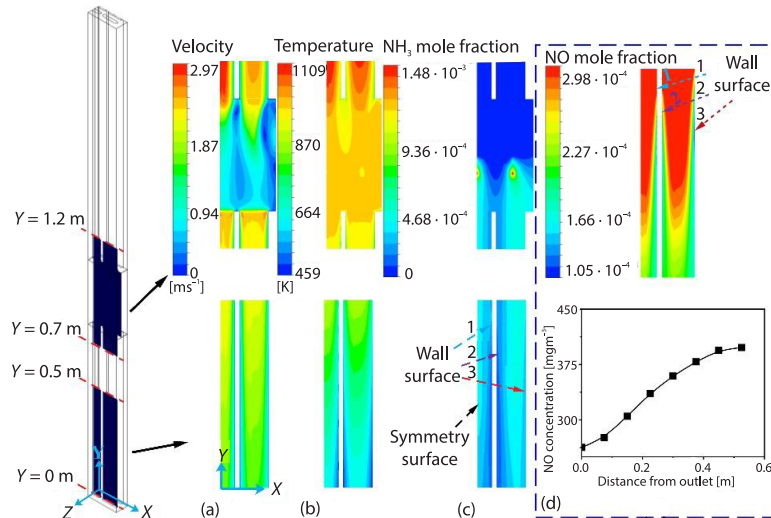

Figure 3. The calculation results of the synergistic SCR catalytic reaction; (a) velocity field, (b) temperature field, (c) NH_3 concentration distribution, and (d) NO concentration distribution

Influence of different parameters on NO reduction in SCR process

This section analyzes the effects of the atomization angle, θ, injection velocity, v, the nozzles number, N, on the flow field uniformity, and NO reduction. In addition, the uniformity index, γ_a, evaluated the NH_3 distribution [10, 11, 33, 35]. The interval $Y = 0\sim800$ mm was selected as the investigation surface for γ_a. The eq. (4) calculated the γ_a of the specific field variable ϕ_i:

$$\gamma_a = 1 - \frac{\sum_{i=1}^{n}\left[\left(\left|\phi_i - \bar{\phi}_a\right|\right)A_i\right]}{2\left|\bar{\phi}_a\right|\sum_{i=1}^{n}A_i} \qquad (4)$$

where ϕ_i is the NH_3 volume concentration on the ith mesh dividing surface, $\bar{\phi}_a$ – the average value of the NH_3 concentration on the entire investigation surface, and A_i – the area of the ith mesh dividing surface. The closer the uniformity index is to 1, the uniformity improves.

Bai, W., *et al.*: Coupling Selective Catalytic Reduction Process inside a Coke ...
THERMAL SCIENCE: Year 2022, Vol. 26, No. 6A, pp. 4571-4582

4577

The effect of the atomization angle on NO reduction

Figure 4(a) shows that increasing the atomization angle has a negligible impact on the NH_3 concentration peak and the NH_3 distribution near *Wall surface-1* and *Wall surface-2*. However, the NH_3 concentration between the adjacent injection points is heightened. Figure 4(b) shows that the atomization angle benefits the uniform distribution of NH_3 at the cross-section. However, the diffusion rate of NH_3 is greater than that of consumption, so the second uniform development is obtained. During the whole process, the uniformity index γ_a was 0.86~0.89, indicating that the NH_3 concentration was preferably distributed.
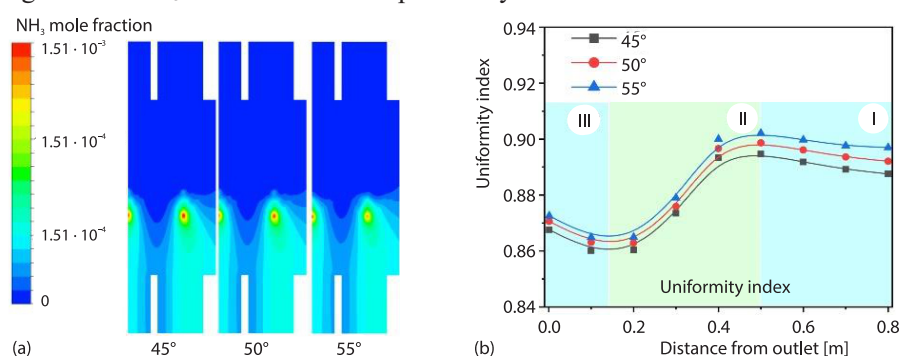

Figure 4. The NH_3 concentration distribution at different atomization angles; (a) the NH_3 distribution in the NH_3 injection space area and (b) the γ_a variation in the catalyst coating area

Figure 5 shows the opposite distribution state on the *Wall surface-2* side and the *Wall surface-3* side of the outer channel. As the investigation area approaches the outlet, this phenomenon gradually weakens. The flue gas carries NH_3 continuously to the exit, which promotes the uniform development of NH_3 in the Y cross-section. Meanwhile, the SCR reaction near the wall also accelerates the diffusion of NH_3 side to side. In the $Y = 200$~0 mm section, the diffusion rate of NH_3 to the *Wall surface-2* side is greater than the consumption rate, which causes the NH_3 concentration increase. Affected by the NH_3 distribution characteristics, *Wall surface-3* shows a sharp decline in NH_3 than *Wall surface-2* at the $Y = 400$~200 mm section.
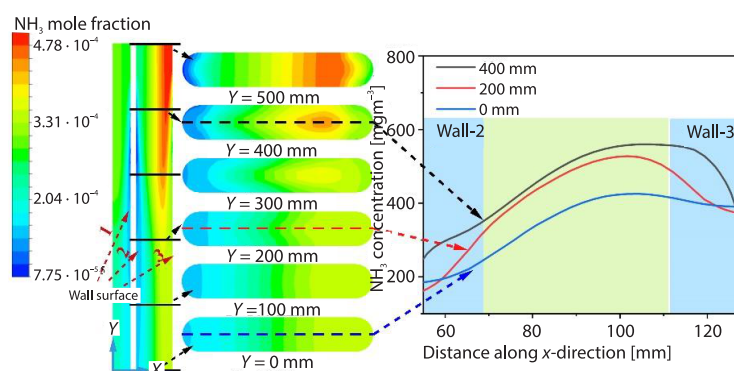

Figure 5. The NH_3 distribution at an atomization angle of 45°

The atomization angles of 45° and 55° correspond to the NO reduction efficiency of 34.4% (reduced to 262.6 mg/m^3) and 34.6% (reduced to 261.6 mg/m^3), respectively. Compared with the initial situation, it increased by 0.4% at most. On the one hand, the variation in the atomization angle was not large enough, and the more important reason was that the catalytic area was too small.

The effect of injection velocity on NO reduction

Figure 6 shows that the NH$_3$ distribution characteristics are similar to the case of atomization angle. The momentum improving the reductant promotes the development of NH$_3$ in the cross-section and the upper part of the NH$_3$ injection space. However, the injection flow was constrained by the mainstream smoke, which also caused the uneven distribution of the *Wall surface*. Compared with the atomization angle, the NH$_3$ concentration noteworthily decreases in the central area and raises near the *Wall surface-2*, whereas the *Wall surface-3* side does not vary significantly. Therefore, further improving the NH$_3$ uniformity benefits the SCR catalytic reaction. From 0.2-0.6 m/s, the outlet NO reduction was 35.5% (reduced to 258.1 mg/m^3) and 36.2% (reduced to 255.1 mg/m^3), respectively. Compared with the initial situation, it increases by 2%. Compared with the case of the atomization angle, it increases by 1.6%. The injection speed has a greater impact on the SCR process than the atomization angle.
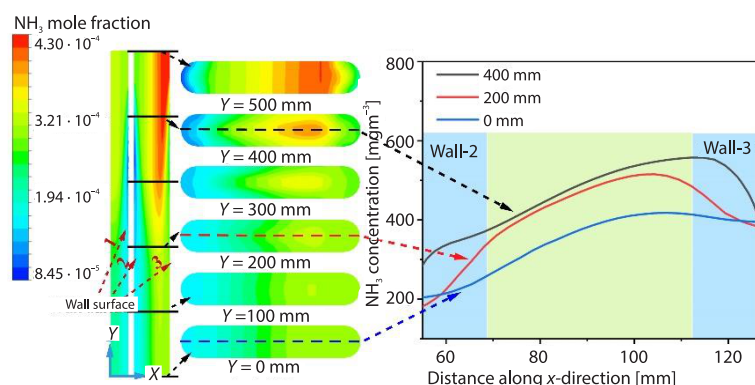

Figure 6. The NH$_3$ distribution at an injection velocity of 0.2 m/s

The effect of the nozzles number on NO reduction

Figure 7 shows the axisymmetric state of the NH$_3$ concentration field gradient decrease under the condition of different nozzle numbers, which confirmed the superior NH$_3$ uniform distribution characteristics. Furthermore, the nozzles number results in a tremendous NH$_3$ distribution increase in *Wall surface-2* along the *X*-direction at $Y = 300$ mm and $Y = 100$ mm than the atomization angle and injection velocity. It is worth noting that the NH$_3$ concentration on the *Wall surface*-2 side is higher than in the center. Concurrently, the NH$_3$ levels of *Wall surface-2* and *Wall surface-3* both drop sharply at the $Y = 300$ mm position, this implies that the ameliorating NH$_3$ concentration near the *Wall surface* is conducive to the SCR catalytic reaction. During the NO reduction process, the consumption rate of NH$_3$ near *Wall surface-2* is greater than the diffusion rate, so that the lessened NH$_3$ cannot replenish, thereby explaining the reason for the distance shortening in the II-zone.

Increasing the number of nozzles the SCR catalytic reaction starting at $Y = 500$ mm and improves NO reduction. From the partially enlarged view at the outlet, it was found that

Bai, W., *et al.*: Coupling Selective Catalytic Reduction Process inside a Coke ...
THERMAL SCIENCE: Year 2022, Vol. 26, No. 6A, pp. 4571-4582

4579

when the nozzles number was 17~25, NO concentration decreased to 256.4~251.6 mg/m³. Compared with the initial working condition, NO reduction increased by 2.9% at the maximum, and it was further increased by 0.9% compared with the injection velocity.
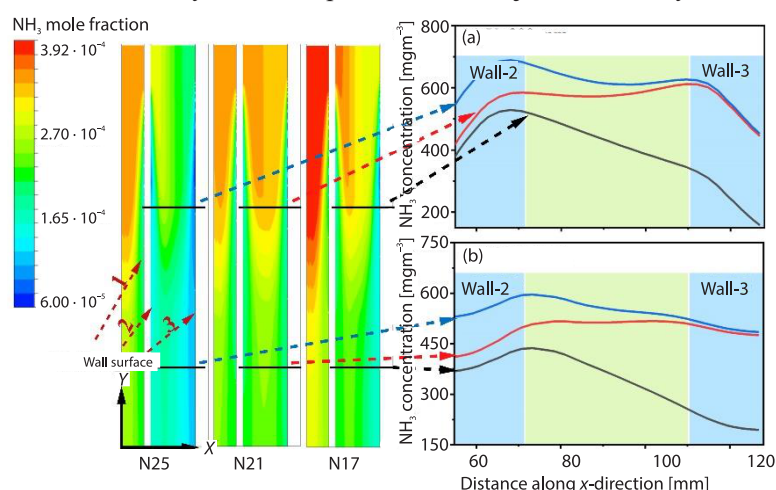

**Figure 7. The NH₃ concentration distribution under the different nozzles number;
(a) the NH₃ distribution at $Y = 300$ mm and (b) the NH₃ distribution at $Y = 100$ mm**

In summary, without adding a mixed flow device, the change of univariate parameters (atomization angle, injection velocity, and the nozzles-number) resulted in 34.4~37.1% of NO reduction (maximum reduction 251.6 mg/m³). It was difficult for the synergistic SCR technology to achieve the standard emission requirement of 150 mg/m³.

The influence of inlet NO concentration on NO reduction

To obtain the NO reduction capacity of the synergistic SCR process in the regenerator, the influence of the inlet NO concentrations of 200 mg/m³ and 150 mg/m³ on the outlet NO concentration was analyzed. Here, an injection velocity of 0.1 m/s, an atomization angle of 40°, and a nozzles number of 25 were adopted. Figure 8 depicts the curve L_1 reflects that the NO concentration reduces by 73.2 mg/m³ in the catalyst coating interval from 500-0 mm, achieving a reduction efficiency of 36.6%. The NO concentration of curve L_2 reduces by 54.6 mg/m³, and a reduction efficiency of 36.4% is achieved. These results show that the outlet NO concentration had less of a relationship with the inlet concentration under given conditions, as determined by the regenerator structure and the SCR coating area. Therefore, it can be inferred that when the inlet NO concentration is less than 235 mg/m³, the application of the cooperative SCR denitration model helps the outlet NO meet the requirements of the emission standard.
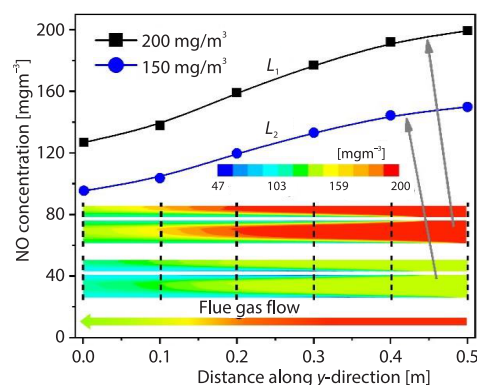

Figure 8. The influence of inlet NO concentration on the spatial NO concentration distribution

Conclusions

- The apparent, uneven distribution of NH_3 concentration developed in the pores. On the one hand, it was caused by the speed difference between the injection flow and the mainstream smoke in the NH_3 injection space. On the other hand, it was determined by the consumption rate of NH_3 participating in the reaction on the catalytic wall and the diffusion rate of NH3 at the center of the wall.
- Increasing the number of nozzles was more helpful than the injection speed and atomization angle in improving the NH_3 distribution near the wall and the NO reduction efficiency. The improvement in the uniformity of NH_3 concentration was mainly due to strengthening the mixing of the injection stream with flue gas in the NH_3 injection space. Without changing the thermal storage brick structure, increasing the mixing effect achieves a maximum NO reduction of 37.1%. When the inlet NO concentration was less than 235 mg/m^3, applying the cooperative SCR reaction model inside the regenerator helped the outlet NO concentration meet the emission standard.

Coating SCR catalyst on the inner lattice brick wall of coke oven regenerator for NO emission reduction has great potential for medium and low temperature SCR denitrification system that replaces coke oven flue gas epitaxy. However, it is necessary to further study and explore whether the thickness of the coated catalyst can obtain better denitration effect, and whether the increase of the coating thickness will affect the heat transfer of the high temperature flue gas-regenerative solid. The next work should be combined with experiments and numerical values to study the operating effects of flue gas-solid coupling heat transfer and SCR catalytic denitration under the harsh conditions of actual production.

Acknowledgment

Nomenclature

A_i – area, [m^2]
A_{NO} – pre-exponential factor, [s^{-1}]
A_{ads} – pre-exponential factor, [m^{3}mol^{-1}]
c_i – species concentration, [–]
$E_{a,NO}$ – activation energy, [kJmol^{-1}]
ΔH_{ads} – adsorption heat, [kJmol^{-1}]
K – adsorption equilibrium constant, [–]
k_{NO} – reaction rate constant, [–]
r_{NO} – NO reaction rate, [–]
T_{in} – inlet temperature, [K]
t – represents time, [s]
u – fluid velocity, [ms^{-1}]

Y – 3-D direction y, [–]

Greek symbols

γ_a – uniformity index, [–]
θ_{NH_3} – coverage rate, [–]
ϕ – field variable, [–]
ϕ_a – average value of the NH_3 concentration, [–]

Acronyms

DPM – discrete phase modelling
SCR   – selective catalytic reduction

References

[1] Diez, M. A., *et al*., Coal for Metallurgical Coke Production: Predictions of Coke Quality and Future Requirements for Cokemaking, *Int. J. Coal. Geol*., *50* (2002), 1-4, pp. 389-412
[2] Du, X., *et al*., Study on Enitrification Catalyst for Coke oven Flue Gas, *Fuel Chem. Proceses*, *2* (2018), pp. 43-47
[3] Jin, K., *et al*., Simulation of Transport Phenomena in Coke oven with Staging Combustion, *Appl. Therm. Eng*., *58* (2013), 1-2, pp. 354-362
[4] Wu, H., *et al*., A Thermal and Chemical Fuel Pretreatment Process for NO$_x$ Reduction from Cement Kiln, *Fuel Process. Technol*., *210* (2020), 15, 106556

Bai, W., *et al.*: Coupling Selective Catalytic Reduction Process inside a Coke ...
THERMAL SCIENCE: Year 2022, Vol. 26, No. 6A, pp. 4571-4582

4581

[5]   Caldeira-Pires, A., *et al.*, Influence of Burner-Port Geometry in Hydrocarbon Oxidation and NO$_x$ Formation Mechanisms in Methane/Air Flames, *Fuel*, *81* (2001), 6, pp. 771-783

[6]   Gamrat, S., *et al.*, Influence of External Flue Gas Re-Circulation on Gas Combustion in a Coke oven Heating System, *Fuel Process. Technol.*, *152* (2016), Nov., pp. 430-437

[7]   Weiss, C., *et al.*, Formation and Control of Nitrogen Oxide in the Heating System of a Coke Oven, *Environ. Eng. Sci.*, *29* (2012), 7, pp. 555-562

[8]   Liu, K., *et al.*, Microkinetic Study of NO Oxidation, Standard and Fast NH$_3$-SCR on CeWO at Low Temperatures, *Chem. Eng. J.*, *423* (2021), 130128

[9]   Muzio, L. J., *et al.*, Overview and Status of Post-Combustion NO$_x$ Control: SNCR, SCR, and Hybrid Technologies, *Int. J. Environ. Pollut.*, *17* (2002), 1-2, pp. 4-30.

[10] Liu, X., *et al.*, Low NO$_x$ Combustion and SCR Flow Field Optimization in a Low Volatile Coal Fired Boiler, *Journal Environ. Manag.*, *220* (2018), Aug., pp. 30-35

[11] Zhang, C., *et al.*, Optimisation Design of SCR Mixer for Improving Deposit Performance at Low Temperatures, *Fuel*, *237* (2019), Feb., pp. 465-474

[12] Liu, H., *et al.*, Optimization and Numerical Simulation of the Flow Characteristics in SCR System, *Energy Procedia*, *17* (2012), Part A, pp. 801-812

[13] Gao, Y., *et al.*, Numerical Simulation and Optimization of Flow Field in the SCR Denitrification System on a 600 MW Capacity Units, *Energy Procedia*, *14* (2012), Dec., pp. 370-375

[14] Mehdi, G., *et al.*, Numerical Investigation of SCR Mixer Design Optimization for Improved Performance, *Processes*, *7* (2019), 3, 168

[15] Ye, J., *et al.*, Numerical Analysis on Enhancing Spray Performance of SCR Mixer Device and Heat Transfer Performance Based on Field Synergy Principle, *Processes*, *9* (2021), 5, 786

[16] Prabhu S. S., *et al.*, Effect of UWS Spray Angle and Positioning of Injector on Ammonia Concentration in Urea-SCR System, *Mater. Today Proc.*, *46* (2021), 17, pp. 8051-8055

[17] Wardana, M., *et al.*, A Study of Urea Injection Timing to Predict the NO$_x$ Conversion in SCR Systems, *Energy Procedia*, *158* (2019), Feb., pp. 1942-1948

[18] Xin, Q., *et al.*, Investigation on Optimal Active Layer Thickness and Sore Size in Dual-Layer NH3-SCR Monolith for low SO$_2$ Oxidation by Numerical Simulation, *Fuel*, *279* (2020), 118420

[19] Zeng, H., *et al.*, Numerical and Experimental Investigations on Reducing Particle Accumulation for SCR-deNO$_x$ Facilities, *Appl. Sci.*, *9* (2019), 4158

[20] Guo, M., *et al.*, Rational Design of Novel CrZrO$_x$ Catalysts for Efficient Low Temperature SCR of NO, *Chem. Eng. J.*, *413* (2021), 127554

[21] Ji, P., *et al.*, Relationship between the Molecular Structure of V$_2$O$_5$/TiO$_2$ Catalysts and the Reactivity of SO$_2$ Oxidation, *Catal. Sci. Technol.*, *4* (2016), 6, pp. 1187-1194

[22] Fang, X., *et al.*, Influence of Surface Active Groups on SO$_2$ Resistance of Birnessite for Low-Temperature NH$_3$-SCR, *Chem. Eng. J.*, *399* (2020), 125798

[23] Guo, K., *et al.*, Conquering Ammonium Bisulfate Poison over Low-Temperature NH$_3$-SCR Catalysts: A Critical Review, *Appl. Catal. B Environ.*, *297* (2021), 120388

[24] Kwon, *et al.*, A Dual Catalytic Strategy by the Nature of the Functionalization Effect as Well as Active Species on Vanadium-Based Catalyst for Enhanced Low Temperature SCR, *Appl. Catal. B Environ.*, *289* (2021), 120032

[25] Yu, J., *et al.*, The Pilot Demonstration of a Honeycomb Catalyst for the DeNO$_x$ of Low-Temperature Flue Gas from an Industrial Coking Plant, *Fuel*, *219* (2018), May, pp. 37-49

[26] Gao, F., *et al.*, Simultaneous Removal of Gaseous CO and Elemental Mercury over Cu-Co Modified Activated Coke at Low Temperature, *Journal Environ. Sci.*, *101* (2021), Mar., pp. 36-48

[27] Zhao, Y., *et al.*, Analysis and evaluation of the Influence of Heat Storage Material on Coke oven Flue Gas Exothermic Process, *Thermal Science*, *25* (2021), 2A, pp. 1095-1108

[28] Lopes, G. C., *et al.*, The CFD Study of Industrial FCC Risers: The Effect of Outlet Configurations on Hydrodynamics and Reactions, *Int. J. Eng. Sci.*, *2012* (2012), ID193639

[29] Zhao, Y., *et al.*, Thermal Process and NO Emission Reduction Characteristics of a New-Type Coke oven Regenerator Coupled with SNCR Process, *Fuel*, *305* (2021), 121510

[30] Zhao, Y., *et al.*, Numerical Simulation of NO Emission Reduction in Coke oven Regenerator with Synergistic SNCR/SCR Process, *E3S Web of Conferences*, *267* (2021), 02053

[31] Ostberg, M., *et al.*, Influence of Mixing on the SNCR Process, *Chem. Eng. Sci.*, *52* (1997), 15, pp. 2511-2525

[32] Koebel, M., Elsener, M., Selective Catalytic Reduction of NO over Commercial DeNO$_x$-Catalysts: Experimental Determination of Kinetic and Thermodynamic Parameters, *Chem. Eng. Sci.*, *53* (1998), 4, pp. 657-669

[33] Bai, W., *et al.*, A Comprehensive Review on Oxygen Transport Membranes: Development History, Current Status, and Future Directions, *Int. J. Hydrogen Energy*, *46* (2021), 73, pp. 36257-36290

[34] Zheng, C., *et al.*, Numerical Simulation of Selective Catalytic Reduction of NO and SO_2 Oxidation in Monolith Catalyst, *Chem. Eng. Sci.*, *361* (2019), Apr., pp. 874-884

[35] Tan, L., *et al.*, The CFD Studies on Effects of SCR Mixers on the Performance of Urea Conversion and Mixing of the Reducing Agent, *Chem. Eng. Process. Process Intensif.*, *123* (2018), Jan., pp. 82-88